Load relief rupture mechanism based on particle flow rocklike material

Peijie Lou[1,2], Shuling Liang[1,*], Mingming Feng[1], Yishun Bu[1], Xinyi Huang[1]

1. School of Civil and Architectural Engineering, Anhui University of Science and Technology, Huainan 232001, China

2. Opening Laboratory for Deep Mine Construction, Henan Polytechnic University, Jiaozuo 454000, China

470474720@qq.com

ABSTRACT. *The purpose of this study was to investigate the microscopic mechanism of rock load relief rupture may be unveiled. The PFC2D meso-structure parameters are calibrated based on a set of results from uniaxial compression test on indoor rocklike materials, and then the particle flow software is used to simulate biaxial compression and load relief tests. Study shows that, in the numerical simulation test of biaxial compression, only a main shear rupture zone forms after the rocklike material is damaged. Local shear rupture zone seems weak; while in the numerical simulation test of load relief, there are multiple shear rupture zones produced after it gets destroyed. The biaxial compression shear rupture zone appears wider than the unload shear rupture zone. from the ratio of the shear cracks to the tensile cracks when unloading, we find that a lot of tensile cracks will generate immediately if suddenly unloaded, so that the tensile failure occurs. subsequently, the shear and tensile cracks remain stable at a certain value, that is, the specimen fails due to the joint tension and shear. the simulation test is conducted with the analysis of the relationship between the uniaxial compression microcracks and the stress, and it is found therefrom that the stress curve of the sample is mainly subjected to change with the number of microcracks. The findings of this study may serve as to avoiding many work accidents have been incurred by work load relief in recent years.*

RÉSUMÉ. *Le but de cette étude était d'étudier le mécanisme microscopique de la rupture de l'allégement de charge rocheuse qui pourrait être dévoilé. Les paramètres de méso-structure PFC2D sont étalonnés sur la base d'un ensemble de résultats d'essais de compression uniaxiale sur des matériaux rocheux d'intérieur, puis le logiciel d'écoulement de particules est utilisé pour simuler des essais de compression biaxiale et de libération de charge. L'étude montre que, dans l'essai de simulation numérique de la compression biaxiale, il ne se forme qu'une zone principale de rupture par cisaillement après l'endommagement du matériau rocheux. La zone de rupture par cisaillement local semble faible; alors que dans l'essai de simulation numérique de l'allégement de la charge, plusieurs zones de rupture par cisaillement sont créées après la destruction. La zone de rupture en cisaillement par compression biaxiale apparaît plus large que la zone de rupture en cisaillement sans charge.*

Annales de Chimie - Science des Matériaux – n° 4/2018, 565-576

Du rapport entre les fissures de cisaillement et les fissures de traction lors du déchargement, nous constatons que de nombreuses fissures de traction seront générées immédiatement en cas de déchargement brutal, de sorte que la rupture en traction se produit. Par la suite, les fissures de cisaillement et de traction restent stables à une certaine valeur, c'est-à-dire que l'éprouvette se déchire du fait de la tension et du cisaillement de l'articulation. Le test de simulation a été réalisé avec l'analyse de la relation entre les microfissures de compression uniaxiales et la contrainte, et l'on constate que la courbe de contrainte de l'échantillon est principalement soumise à une modification avec le nombre de microfissures. Les résultats de cette étude pourraient permettre d'éviter que de nombreux accidents de travail aient été causés par un allégement de la charge de travail au cours des dernières années.

KEYWORDS: *Particle flow, unload, mesoscopic rupture mechanism.*

MOTS-CLÉS: *flux de particules, dechargement, mecanisme de rupture mesoscopique.*

DOI:10.3166/ACSM.42.565-576 © 2018 Lavoisier

1. Introduction

In general, geotechnical works involves the heaped loading and unloading processes. Till now, the loading (heaped loading) rock mass mechanics has been widely studied with a suite of theories that reflect the deformation and failure of the rock mass under the load paths. In this regard, unloading stress paths go the other way around. Both loading and unloading processes cause rock mass to appear different deformations and failure characteristics whether in mechanical mechanism or in mechanical response (Huang *et al.*, 2009; Zhang, 2009; Fan *et al*., 2011).

In recent years, many work accidents have been incurred by work load relief, such as: the bottom heave caused by unloading during foundation pit excavation, bass drum, roof collapse and collapse of the wall rock caused due to unloading during the cavern excavation.

Huang and Huang, (2008) explored the full process of stress-strain curve and fracture characteristics of rock under unloading conditions based on the rock specimen load relief test. Huang *et al*., (2010) also analyzed this full process by the unloading test under high confining pressure and the constitutive equation was available for the appropriate segment according to the characteristics in each phase. Many scholars (Li *et al*., 2010; Chen *et al*., 2010; Xia *et al*., 2009; Zhang *et al*., 2011) have made extensive studies on the macro-mechanical properties, deformation characteristics, constitutive equations and fracture mechanism of rock load relief, and borne satisfactory fruits. However sadly, in the field of the meso-structure fracture mechanism, they are just getting started.

The high nonlinearity and anisotropy of the jointed rock masses will attribute to time-consuming and costly laboratory tests, and the test results are highly non-reproducible. In recent years, the PFC, a numerical simulation software in the direction of rock (mass), has risen rapidly for exploring the mechanical properties and behaviors of medium from the perspective of meso-structure, so in an attempt to reveal the essence of substances (Luo, 2007). This paper, based on the particle flow

PFC2D, conducts the numerical simulation test on loading and unloading processes in order to reveal the rock rupture mechanism from this angle.

This paper includes six sections: Introduction, Lab test, Determination of mesostructured parameters of PFC2D, Analysis of the relationship between the microcracks and stress, Rocklike unloading simulation test, Conclusions.

2. Lab test

Here, cement mortar is used to simulate rock. The material is mixed as follows: ordinary Portland cement (R325): less than 2.5mm particle diameter: medium sand: water = 1:1.5:0.5. In order to obtain the mechanical properties of similar rocklike materials, the PFC2D can be used to calibrate the parameters in order to provide the clues to this. The uniaxial compression test is carried out on the matching material specimen by using the RMT-150B test system. The loading mode uses the displacement control with ramp type waveform at 0.0020 mm/s. In order to more accurately measure the horizontal axis and vertical deformations of the specimen itself, a plastic base strain gauge of 20 mm × 3 mm grid width is added horizontally and vertically in the middle of the specimen, respectively.

Figure 1. Strain gauge paste diagram

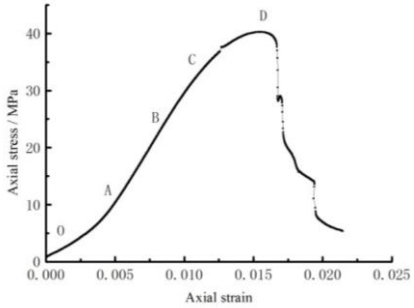

Figure 2. Uniaxial compression indoor test stress-strain curve of rock-like

The full stress-strain curve of the rocklike specimen under uniaxial compression loads (Fig.2) is very similar to the typical full stress-strain curve of the rock. It can also be divided into the five phases, i.e. compaction (OA) and the elasticity (AB), fissure burgeon and stable expansion (BC), the unsteady development of the crack until the rupture (CD), and the strain softening, which reproduce the hard brittleness and dilatancy of the rock.

3. Determination of mesostructured parameters of PFC2D

The parallel bond model can well reflect the mechanical properties of rock materials (Shi and Xu, 2015). In this simulation test, the rocklike material uses the parallel bond model. With trial-and-error method, the meso-parameter parameters of Table 1 are used to simulate this uniaxial compression test of the rocklike materials after repeated iteration.

Table 1. PFC2D simulation sample meso parameters

Parameter	Value
Specimen width/mm	50
Specimen height/mm	100
Particle density/（$kg \cdot m^{-3}$）	2312
Particle minimum radius/mm	0.3
Particle size ratio	1.66
Particle contact modulus/GPa	3.8
Particle stiffness ratio	3.2
Parallel bond radius multiplier	1.0
Parallel bond modulus/GPa	3.8
Parallel bond stiffness ratio	3.2
Particle friction coefficient	0.25
Parallel bond normal strength /MPa	29±3.5
Parallel bond tangential strength /MPa	39±4.75

The simulation is loaded in the displacement control mode with axially loaded plate at 0.09m/s. In order to show that it is still quasi-static in the PFC simulation software at a load speed of 0.09m/s, a history command is used to monitor the work (boundary energy) done during loading with plate, which is then compared to the total strain energy (also monitored by the history command) stored in the particle set. In the elastic phase of the test, if the two energies are equal, it shows that the loading

speed is reasonable (quasi-static); if they are not equal or prematurely separated, it indicates that the work done by the loading plate on the component accesses the component's kinetic energy prematurely (consumed by the damping mechanism built-in PFC). A curve of the total strain energy and boundary energy-axial strain simulated in the test is shown in Fig. 3, which well illustrates that the simulation test is still quasi-static.

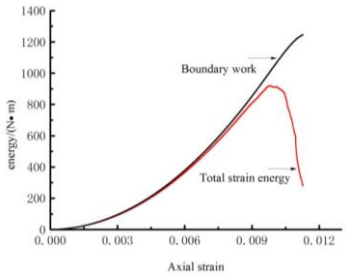

Figure 3. Energy-axial strain diagram of the specimen

The comparison between the simulation results and the stress-strain curves obtained in the laboratory test is shown in Fig. 4, where the uniaxial compression strength of the rocklike material is 40.27 MPa, while it is 40.05 MPa by PFC simulation. There is a deviation of 0.55% between both. The elastic moduli of rock-like material tested in the lab and by PFC are 3.87 GPa and 3.94 GPa, respectively, with a deviation of 1.81%. The Poisson's ratios obtained in the lab and by PFC simulation are 0.26 and 0.28, respectively, with a deviation of 7.69%. As above, it follows that the macro-mechanical parameters of the rocklike materials obtained by the above-mentioned PFC meso-structure parameter simulation are very similar to the indoor test results of the materials. It should be noted that the appropriate strain at the peak in PFC numerical simulation is 0.98×10^{-2}, while 1.53×10^{-2} in the laboratory test, which are quite different because the initial aggregation of compaction has generated in the first step of PFC modeling, and the floating particles are eliminated in the third step, so that there is no typical "notch curve" that the indoor rocklike sample may appear" (initial compaction phase).

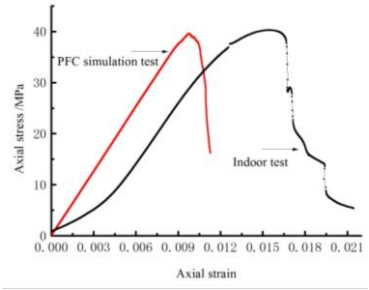

Figure 4. Comparison of stress-strain curve simulation and indoor test of sample

A comparison between the final fracture modes obtained from the lab and the PFC simulation tests is shown in Fig. 5. It is obvious that when the rocklike material is uniaxially compressed in the lab test, axial splitting damage occurs mainly in the upper and lower sections of the specimen, and shear failure occurs mainly in the middle part. In addition, a "Y" crack appears in the upper loading section of the specimen and seems very similar to the PFC simulation results, which shows that the selection of the meso-structure parameters is reasonable because it can reproduce the macro-response of the simulated object.

4. Analysis of the relationship between the microcracks and stress

Figure 6 gives a uniaxial compression stress-strain curve and the microcrack number-strain curve of PFC simulation. At the initial stage of loading, there is almost no damage in the specimen due to the low pressure, so that microcrack does not appear. The stress-strain almost remains linear, pertaining to a completely elastic state (origins O through A). The slope of the stress-strain curve in the AB segment is slightly lower than that in the OA segment, and the slope of the whole segment remains substantially constant. Microcracks generate after point A, and the slope of the microcracks-strain curve from points A to B does not change significantly, and roughly remains constant. The slope of the stress-strain curve in the BC segment tumbles to a certain extent, that is, it has a certain change. After B point, the number of microcracks suddenly increases rapidly and the slope suddenly beefs up. The peak stress after point C swoops, while the number of corresponding microcracks increases quickly. It is then concluded that the change in the slope of the stress-strain curve is negatively correlated with that in the microcracks-strain. That is to say, the number of microcracks increases significantly every time the stress curve has a significant fall, and there is a growth spurt in the cumulative curve of microcracks. It can be regarded that the stress-strain curve of the specimen is subjected to change with the number of microcracks.

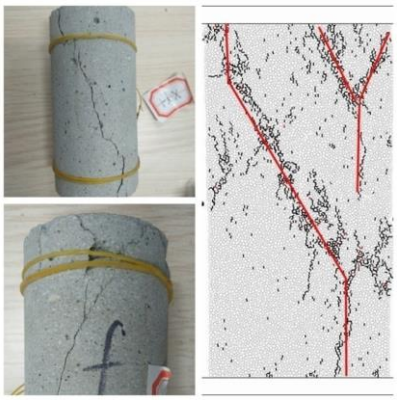

Figure 5. Comparison of the final rupture pattern between laboratory test and PFC2D simulation test

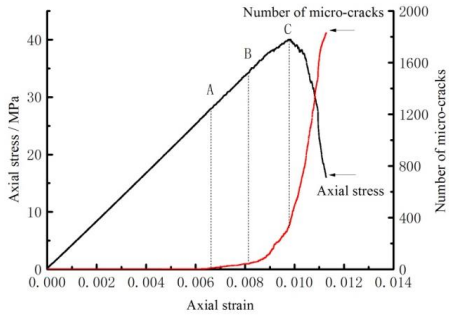

Figure 6. Curve of axial stress - axial strain - microcracks

5. Rocklike unloading simulation test

For the sake of comparison, a constant 20 MPa confining biaxial compression test is performed prior to unloading.

You, (2000) stated that in rock works, if the stress in one direction reduces and after the rock is subjected to yield failure, the adjustment will occur in stress state to establish a new balance. That is to say, after the stress in one direction is reduced, the stress in the other direction falls down accordingly, rather than increases or remains unchanged. For this purpose, the axial pressure and confining pressure reliefs are designed in parallel. The unloading speeds for confining and axial pressures herein are 4.5e-1m/s and 9.0e-3m/s, respectively. In order to distinguish the successive unloading sequence of confining and axial pressures, the concrete procedure includes three phases:

1. Gradually apply to a predetermined value (20 MPa) according to hydrostatic pressure conditions;

2. The confining pressure remains unchanged, gradually increase to a certain stress state before the rock sample is destroyed (85% of the biaxial compression peak stress);

3. Unload the confining pressure at 4.5e-1m/s and the axial pressure at 9.0e-3 m/s, the termination condition is 0.7 times the peak value of the axial stress.

Additionally, in order to fully explain that the macro- and meso-structure properties of rocklike materials in the whole process derive from confining pressure relief, we also design a comparative test in this simulation, as shown below: the first and second steps are given as above. The third step is to relieve the axial pressure at 9.0e-3 m/s alone under the constant confining pressure of 20 MPa, and the termination condition is 0.7 times of the axial stress peak.

The axial stress-strain curve swoops after unloading. Axial strain is roughly divided into two phases (Figure 7), i.e. the strain micro-rebound phase, when the

confining pressure relief runs quickly, axial load is also relieved at a small speed (the upper loading plate moves up and the lower loading plate moves down), so that the strain rebound occurs; and axially continuous and increasing compression, this is because the lateral strain rapidly expands at a gradually increasing rate. The lateral expansion under the Poisson effect inevitably causes axial contraction. The axial strain converts into axial compression when the axial contraction is greater than the resilience value caused by axial load relief. It can be seen that the specimen exhibits obvious brittleness and expansion characteristics. In addition, Fig. 7 also gives the microcracks-axial strain curves of the load relief scheme and the proof scheme. As shown in the figure, we know that a lot of microcracks generate during the load relief process.

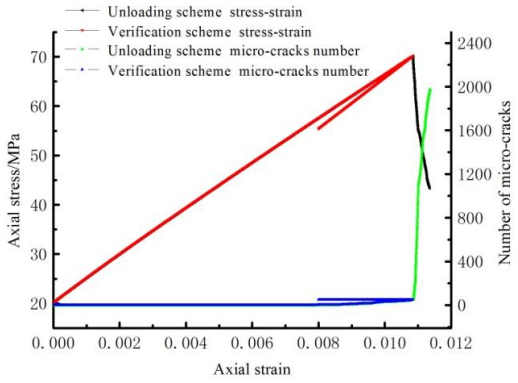

Figure 7. Curve of axial stress - axial strain - microcracks

5.1. Comparison among three stress paths of rock-like

In this section, we compare and analyze the results from the numerical simulation on rupture mode and fracture mechanism of rock-like materials under three stress paths.

As shown in Fig. 8, the crack form of the rock-like specimen at failure presents under the biaxial compression (Figure a) and load relief (Figure b). In the numerical test of biaxial compression, only one main shear rupture zone is formed after the rock sample is damaged, and the local shear rupture zone is not obvious; while in the numerical test of unloading, multiple shear rupture zones generate after the rock sample is damaged. It is difficult to differentiate the primary and secondary shear rupture zones from the whole; the width of the shear rupture zone in the numerical test of loading is greater than that in the numerical test of unloading.

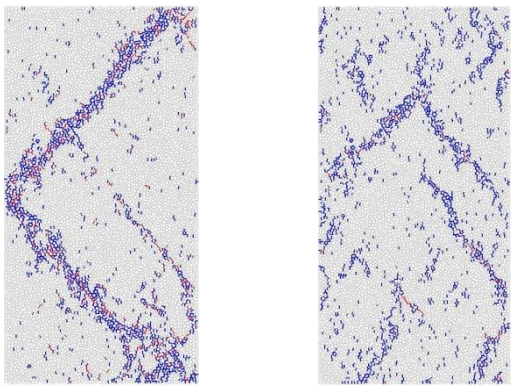

(a) (b)

Figure 8. Specimen crack shape diagram at the time of final destruction

As shown in Figure 9, the parallel bond stress is distributed in a chain (the red represents parallel bond tensile stress) in the specimen after the final failure under the biaxial compression (a) and unloading (b) tests of the rock-like specimen. It is obvious that the parallel bond tensile stress at failure in the specimen in the unloading test is significantly greater than that in the confining pressure relief test.

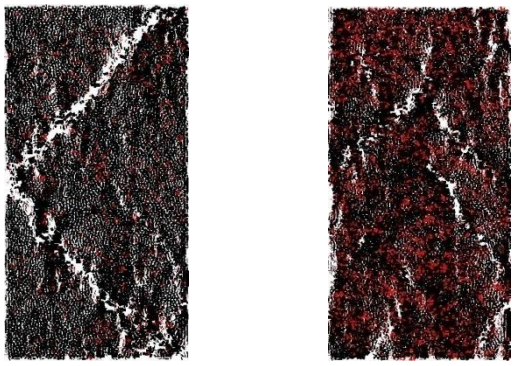

(a) (b)

Figure 9. Distribution of parallel cohesive force chains at final failure of test specimens

Figure 10 is the ratio of shear fissures to tensile cracks in microcracks under three stress paths.

As shown in Figure (a), the tensile microcracks first generate during uniaxial compression. Only when the total number of microcracks increases rapidly will the

shear cracks appear. Then the ratio of shear to tensile cracks rises wavelike, but is always lower, up to approximately 2.0%

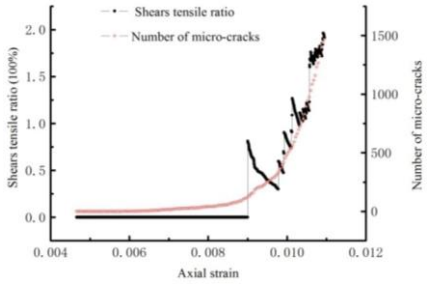

(a) Curve of ratio of shear and tensile microcracks under uniaxial compression

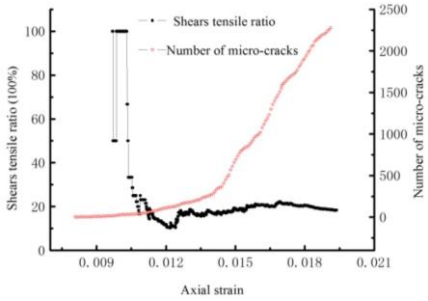

(b) Curve of ratio of shear and tensile microcracks under biaxial compression

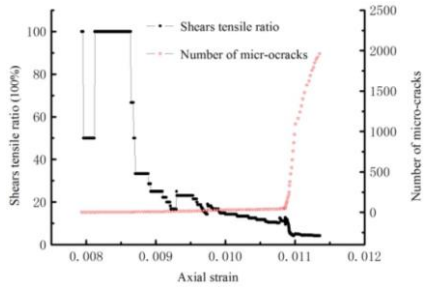

(c) Curve of ratio of shear and tensile microcracks under load relief

Figure 10. PFC simulation and tension crack ratio variation diagrams of three stress paths

As shown in Figure (b), the shear crack occurs first under the biaxial compression, and the tensile crack then generates and proliferates rapidly. At last, the ratio of the shear cracks to the tensile cracks remains stable at about 20%

As shown in the Figure (c), when the test runs to the unloading phase, the tensile crack increases suddenly, and then the ratio of the shear cracks to the tensile cracks remains at about 5%. It can be seen that the tensile failure of the specimen occurs when the load is suddenly removed. The specimen is damaged under joint tension and shear. It should be noted that, in the pursuit of consistency between fracture morphologies under simulation and laboratory tests, the parallel bond normal strength should be lower than the parallel bonding tangent strength when calibrating the meso-structure parameters. It is believed that it is one cause of why the ratio of shear cracks to tensile cracks in the three paths is always lower.

6. Conclusions

1. During the simulation, the particles in the rock-like material move under the exogenic action, so that the contact force between the particles is greater than the parallel bond strength. The parallel bond fracture generates microcracks which expand to cause the stress change with the strain. To be specific, when the curve of microcracks has a significant increase, the stress-strain curve corresponds to a more significant sink;

2. The ratio of shear crack to tensile crack during biaxial compression and unloading tests, it is found that when the ratio of shear cracks to tensile cracks in the specimen swoops to a certain value during sudden unloading, that is, a lot of tensile cracks suddenly generate, the tensile failure occurs; while this ratio remains at a certain value, the specimen fails under joint destroy from tension and shear.

Acknowledgments

This work is supported by Opening Laboratory for Deep Mine Construction, Henan Polytechnic University (2015KF-05);Anhui Provincial Natural Science Foundation (1608085QE122); China Postdoctoral Science Foundation (2016M590558); The Open Project Program Foundation of Engineering Research Center of underground mine construction, Ministry of Education(Anhui University of Science and Technology) (2015KF04); National College Students' Innovation and Entrepreneurship Training Program (201710361027); National College Students' Innovation and Entrepreneurship Training Program (201710361029)

Reference

Chen W. Z., Lü S. P., Guo X. H., Qiao C. J. (2010). Unloading confining pressure for brittle rock and mechanism of rock burst. *Chinese Journal of Geotechnical Engineering*, Vol. 32, No. 6, pp. 963-969.

Fan Y. B., Wu F. Q., He H. F., Ren A. W. (2011). Experiment research about mechanical characteristic of gneissic granite while confining pressure is unloaded. *Hydrogeology & Engineering Geology*, Vol. 38, No. 3, pp. 54-58. http://doi.org/10.3969/j.issn.1000-3665.2011.03.010

Huang S. W., Si T. H., Feng J. W., Cao Y. Q. (2009). Analysis of surrounding rock pressure of Niuhushan tunnel under unloading effect. *Chinese Journal of Underground Space and Engineering*, Vol. 5, No. 1, pp. 79-84. http://doi.org/10.3969/j.issn.1673-0836.2009.01.015

Huang W., Shen M. R., Zhang Q. Z. (2010). Study of unloading dilatancy property of rock and its constitutive model under high confining pressure. *Chinese Journal of Rock Mechanics and Engineering*, Vol. 29, No. S2, pp. 3475-3481.

Hunag R. Q., Huang D. (2008). Study on deformation characteristics and constitutive model of rock on the condition of unloading. *Advances in Earth Science*, Vol. 23, No. 5, pp. 441-447. http:// doi.org/10.3321/j.issn:1001-8166.2008.05.001

Li J. L., Wang R. H., Jiang Y. Z., Liu J., Chen X. (2010). Experimental study of sandstone mechanical properties by unloading triaxial tests. *Chinese Journal of Rock Mechanics and Engineering*, Vol. 29, No. 10, pp. 2034-2041.

Luo Y. (2007). Simulation of soil mechanical behaviors using discrete element method based on particle flow code and its application. *Zhejiang University*.

Shi C., Xu W. Y. (2015). Technique and practice of numerical simulation of particle flow. Beijing, *China Architecture & Building Press*.

Xia C. C., Yan Z. J., Wang X. D., Zhang C. S., Zhao X. (2009). Research on elastoviscosity constitutive relation of marble under unloading condition. *Chinese Journal of Rock Mechanics and Engineering*, Vol. 28, No. 3, pp. 459-466.

You M. Q. (2000). Strength and deformation of rock specimens. *Beijing: Geological Publishing House.*

Zhang L. M. (2009). Experimental and theoretical study on macroscopic and mesoscopic failure mechanism of rock mass under loading and unloading conditions. *Xi`an University of Architecture and Technology*.

Zhang L. M., Wang Z. Q., Shi L. (2011). Experimental study of hard rock failure characteristic under unloading condition. *Chinese Journal of Rock Mechanics and Engineering*, Vol. 30, No. 10, pp. 2012-2018.